Oral Presentation

The 7th TSME International Conference on Mechanical Engineering
13-16 December 2016

TSME ICOME 2016
Mechanical Engineering Innovation for Green Society

DRC0005

STICK-SLIP FRICTION COMPENSATION FOR VISION SERVO TRACKING OF AN AUTOMATED PIPETTE INJECTION WITH SOLENOID VALVE ACTUATOR BY SLIDING MODE WITH ADAPTIVE PI TUNING

Tossaporn Chamsai [1], Nantiwat Pholdee[3], Papot Jaroenapibal[2], and Thana Radpukdee [2,*]

[1] Department of Industrial Technology, Faculty of Industrial Education, Rajamangala University of Technology ISAN Khon Kaen Campus, 46000, Thailand
[2] Department of Industrial Engineering, Faculty of Engineering, Khon Kaen University, 40000, Thailand
[3] Department of Mechanical Engineering, Faculty of Engineering, Khon Kaen University, 40000, Thailand
[*] Correspon\ding Author: tthanar@gmail.com, rthana@kku.ac.th, Tel. 081-2624949, Fax. 043-347227

Abstract

The main goal of this study is to develop an advanced control system for compensation of a stick-slip friction problem in the vision servo tracking of an automated pipette injected with a solenoid valve actuator. In the control framework, the sliding mode control (SMC) technique is incorporated with a new adaptive PI controller. The advantage is that the adaptation law is capable of updating the PI controller online during the control procedure within a short period, while the robust performance is similar to that of the sliding mode. For the stability of the closed-loop control, it is guaranteed in the sense of Lyapunov's direct method. Simulation results reveal that the proposed controller can attain an excellent control performance with can compensate the stick-slip friction effect, while the pipette can closed-to the desired position very well, smoothing movement, high robustness, and high accuracy.

Keywords: an automated pipette, robust adaptive control, stick-slip friction

1. Introduction

In a biological injection technology of a vision-servo system [1, 2], a position control of an auto-mated pipette injection plays an important role in a biomanipulator [3-5]. For genetically modified an organism, a human operator during cellular injection can partially substituted with an automated injection manipulator which can present more accuracy and tiny inaccuracies. In a practice, the de-sired position can be obtained from the space coordinate which obtained by recognizing the distances of an indicator [6], thereby a high-precision position control of an actuator is a crucial when the manipulators are stirred to the desired position in a microscopic level. For development of methodologies for the automated pipette system in which direct driven by a fluid power, a solenoid valve is one of the actuator which has been widely applied for pressure/flow control of the fluid source. Because actuated with the solenoid valve can offers the advantages of high accuracy, low-cost, and simple in a practice [7]. Unfortunately, actuated with the solenoid-valve often possesses undesirable characteristics from uncertain nonlinearities which are presented in the mechanism system for a particular the stick-slip friction effect [7, 8] which has led to deteriorate the precision of the position control during the pipette is applied in the microscopic level [9]. In the im-plementation, the friction effect depends on both the interface properties of interacting surfaces and on the dynamics of the system; therefore, an interest response in a typical direction is not normal to smooth as the discontinuous effect. As the results, the precision of position control in microscopic process can be deteriorated [11-14]. To do this, many advanced control system have been widely developed which proposed to increase the precision control of the actuator in the automated pipette injection system.

In much control system, the sliding mode control (SMC) method is one of the control technique to dominate the parametric uncertainties and external disturbances, while the control principle is not require the precise of system modeling [10-12]. Nevertheless, if sliding mode exists, the chattering phenomenon of the control input can cause decreasing the control accuracy when sliding mode application [13, 14]. In [15-17], an adaptive control approach is widely applied into the SMC. An adaptive PI control technique is one of the adaptive control approaches which commonly combined in many control application [18, 19]. The flexibility of the PI tuning lies in the specification of the PI gains in which using the error signals in order to realize the online adjustable gains during a control process and is capable of adjusted online according to the adaptation laws [20-23]. By incorporated with the adaptive PI control, an inaccuracy can be improved, while the robust performance can be preserved by the act of the sliding mode [18].

For our knowledge, this only identifies systems which a human operator during cellular injection can replaced with an automated injection manipulator. Therefore, in this study, the SMC with a new adaptive PI controller is proposed to realize the highly-accurate motion control in microscopic level application of the solenoid valve actuator, which is used for direct actuated the motion control of the automated pipette injection in the fluid power drives system. The performance of the proposed controller design was assessed with the stick-slip friction effect which is a critical problem of the motion control in tiny scale. The remainder of this paper is organized as follows. Firstly, we present the proposed controller design. In section 3, a description of the system modeling is presented. In section 4, the simulations results are presented to verify the effectiveness of the development control approach. Finally, the research conclusions are presented.

2. CONTROLLER DESIGN

2.1 System condition

An automated pipette is an application of position control using a solenoid valve. Many works [24-27] about the solenoid valves and pistons with the stick-slip phenomena have been studied. Its system according to those works comprise of the second-order equation of the solenoid valve actuator and the piston, the flow and pressure relation along its component, and flux-current relation within the electromagnetic system. In practice, the system can be assumed to be a first-order system similar to the work of [24-27]. For simplicity, let the system is considered as a first-order uncertain nonlinear system, satisfying uncoupling and matching conditions [28, 29] and can be defined as

$$\begin{aligned} \dot{\mathbf{x}}(t) &= \mathbf{f}(\mathbf{X},t) + \mathbf{b}(\mathbf{X},t)\mathbf{u}(t) + \mathbf{b}(\mathbf{X},t)\boldsymbol{\delta}(\mathbf{X},t) \\ \mathbf{x}(t_0) &= \mathbf{x}_0 \end{aligned} \tag{1}$$

where $\dot{\mathbf{x}} = [\dot{x}_1, \dot{x}_2, \dot{x}_3, \dots, \dot{x}_m]^T \in R^m$ which is the 1st-order of the state vector, t is time, $\mathbf{f}(\mathbf{X},t) = [f_1, f_2, f_3, \dots, f_m]^T \in R^m$ which is known nonlinear function, $\mathbf{X}$ is the global state vector for the nonlinear system and $\mathbf{X} = [x_1, x_2, x_3, \dots, x_m]^T \in R^m$, m is the number of the independent coordinates of x_i, $i = 1,2,3, \dots, m$, $\mathbf{u}(t)$ is the control input and $\mathbf{u}(t) = [u_1, u_2, u_3, \dots, u_m]^T \in R^m$, $\boldsymbol{\delta}(\mathbf{X},t)$ is the uncertain element that presents only in the highest order of the system and $\boldsymbol{\delta}(\mathbf{X},t) = [\eta_1, \eta_2, \eta_3, \dots, \eta_m]^T \in R^m$, and $\mathbf{b}(\mathbf{X},t)$ is the control gain distribution matrix which is positive definite in all arguments and $\mathbf{b}(\mathbf{X},t) = [b_{ij}] \in R^{m\times m}$, $i,j = 1,2,3, \dots, m$. The aim is to force the system state $\mathbf{x}$ to reach the desired state $\mathbf{x_d}$ so that the error $\tilde{x}_i = x_i - x_{id} \to 0$, and $i = 1,2,3, \dots, m$. Not only does a control law have to steer the response closed to the desired value, but it must be the capability to overcome a system's uncertainties.

In order to design the proposed controller, the assumptions below in which correspond to the work of [30] are used for control law derivation which will be expressed in the next section.

Assumption 1: Let $\mathbf{f}(\mathbf{X},t)$, $\mathbf{b}(\mathbf{X},t)$, and $\boldsymbol{\delta}(\mathbf{X},t)$ are continuously differentiable and continuous in $\mathbf{X}$ for all time (t), and $\boldsymbol{\delta}(\mathbf{X},t)$ is within the range space of $\mathbf{b}(\mathbf{X},t)$.

Assumption 2: $\mathbf{b}(\mathbf{X},t)\boldsymbol{\delta}(\mathbf{X},t)$ is upper bounded with $\|\mathbf{b}(\mathbf{X},t)\boldsymbol{\delta}(\mathbf{X},t)\| \le K_O$, and $d(\mathbf{b}(\mathbf{X},t)\boldsymbol{\delta}(\mathbf{X},t))/dt$ is upper bounded by $\|d(\mathbf{b}(\mathbf{X},t)\boldsymbol{\delta}(\mathbf{X},t))/dt\| \le K_d$, and given K_d and K_O are known constants.

Assumption 3: $0 < b_{lower} \le \|\mathbf{b}(\mathbf{X},t)\| \le b_{upper}$ is the bound of the input matrix and its derivative is upper bounded by $\|d(\mathbf{b}(\mathbf{X},t))/dt\| \le b_d$, and given b_{lower}, b_{upper}, and b_d are known constants.

2.2 Robust adaptive PI controller design

To derive the proposed control law in this work, the conception of the robust sliding mode control theory is applied [31]. With the control theorem, the sliding function [29] is adapted to the 1st-order system.

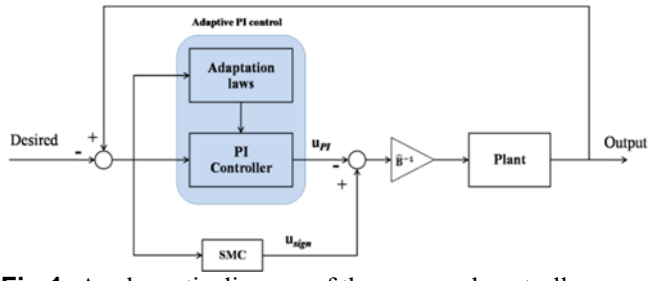

Fig 1: A schematic diagram of the proposed controller.

Consequently, the sliding function can be expressed on each state as

$$\sigma_{it}(x_i(t)) = \tilde{x}_i, \quad i = 1,2,3, \dots, m \tag{2}$$

Thereby, the sliding function and its first derivative of Eq. (1) can be expressed as following

$$\boldsymbol{\sigma}_t(\mathbf{x}) = \mathbf{x} - \mathbf{x}_d \tag{3}$$

And

$$\dot{\boldsymbol{\sigma}}_t(\mathbf{x}) = \boldsymbol{C}(\dot{\mathbf{x}} - \dot{\mathbf{x}}_d) \tag{4}$$

where $\boldsymbol{\sigma}_t(\mathbf{x})$ has components satisfying the sliding function stated earlier and $\boldsymbol{\sigma}_t(\mathbf{x}) = [\sigma_{1t}, \sigma_{2t}, \sigma_{3t}, \dots, \sigma_{mt}]^T$, let $\boldsymbol{C}$ is a positive constant coefficient $m \times m$ matrix. From Fig. 1, the control input is

$$\mathbf{u}(t) = \hat{\mathbf{b}}^{-1}\mathbf{u}_{sign} - \hat{\mathbf{b}}^{-1}\mathbf{u}_{PI} \tag{5}$$

where $\mathbf{u}_{sign} = -\boldsymbol{K}_{sign}\mathbf{sign}(\boldsymbol{\sigma})$, which $\mathbf{u}_{sign}$ is the switching signal and $\text{sign}(s_i) = \begin{cases} +1 & if \ \sigma_i > 0 \\ -1 & if \ \sigma_i < 0 \end{cases}$. Given $\boldsymbol{K}_{sign} = diag(K_O|\sigma_{it}|)$, $\mathbf{sign}(\boldsymbol{\sigma}) = [\text{sign}(\sigma_1), \text{sign}(\sigma_2), \text{sign}(\sigma_3), \dots, \text{sign}(\sigma_m)]^T$, and the control

DRC0005

signal of the adaptive PI tuning is $\mathbf{u}_{PI}$. For $\mathbf{u}_{PI}$, it can be obtained by

$$\mathbf{u}_{PI} = \mathbf{k}_P\mathbf{s} + \mathbf{k}_I \int \mathbf{s}dt \tag{6}$$

where $\mathbf{k}_P$ is the proportional gain and let $\mathbf{k}_P = \text{diag}(k_{Pi})$ and $\mathbf{k}_I$ is the integral gain, and let $\mathbf{k}_I = \text{diag}(k_{Ii})$, while k_{Pi} and k_{Ii} are not equal to zero.

With the Lyapunov's theorem, it is chosen in order to prove the stability of the proposed control system. In addition, with the assumption 3, it can be extended to the gain margin concept [29] which is applied for the adaptation law derivation. Consequently, if the Lyapunov function candidate is $\mathbf{V} > 0$, $\dot{\mathbf{V}}$ can be obtained as

$$\mathbf{V} = \frac{1}{2}\mathbf{s}^T\mathbf{s} + \frac{1}{2}\mathbf{k}_P^T\mathbf{k}_P + \frac{1}{2}\mathbf{k}_I^T\mathbf{k}_I \tag{7}$$

Then, the first-derivative of Eq. (7) can be expressed as

$$\dot{\mathbf{V}} = \boldsymbol{\sigma}^T\dot{\boldsymbol{\sigma}} + \mathbf{k}_P^T\dot{\mathbf{k}}_P + \mathbf{k}_I^T\dot{\mathbf{k}}_I \tag{8}$$

To obtain the Lyapunov stability, substituted $\dot{\boldsymbol{\sigma}}$ into Eq. (8) yields to

$$\dot{\boldsymbol{\sigma}} = \boldsymbol{C}(\dot{\mathbf{x}} - \dot{\mathbf{x}}_d) \tag{9}$$

$$= \boldsymbol{C}(\mathbf{f} + \mathbf{b}\boldsymbol{\delta} - \dot{\mathbf{x}}_d) + \boldsymbol{C}\frac{\mathbf{b}}{\hat{\mathbf{b}}}(-\mathbf{f} + \dot{\mathbf{x}}_d - \mathbf{u}_{PI}) \tag{10}$$

$$= \left(\boldsymbol{C}\mathbf{f} + \boldsymbol{C}\mathbf{b}\boldsymbol{\delta} - \boldsymbol{C}\frac{\mathbf{b}}{\hat{\mathbf{b}}}\mathbf{f}\right) + \boldsymbol{C}\left(\frac{\mathbf{b}}{\hat{\mathbf{b}}} - 1\right)\dot{\mathbf{x}}_d - \boldsymbol{C}\frac{\mathbf{b}}{\hat{\mathbf{b}}}\mathbf{k}_P\boldsymbol{\sigma} \tag{11}.$$

As seen in Eq.(11), due to the control gain $\mathbf{b}$ cannot be determined exactly. Consequently, the conception of the gain margins [29] is applied in this work, and the gain estimation can be considered as $\hat{\mathbf{b}}$=diag($\hat{b}$) where $\hat{b} = \sqrt{b_{lower}.b_{upper}}$, which the bound of the control gain ratio can be defined by $\beta^{-1} \leq \left\|\frac{\hat{\mathbf{b}}}{\mathbf{b}}\right\| \leq \beta$. Let $\beta = \sqrt{\frac{b_{upper}}{b_{lower}}}$ and the initial value in each argument of $\mathbf{k}_P$ and $\mathbf{k}_I$ are positive. Then lets Eq.(8) is substituted with Eq. (11). Thus,

$$\dot{\mathbf{V}} = \boldsymbol{\sigma}^T\left[\boldsymbol{C}\left(\mathbf{f} + \mathbf{b}\boldsymbol{\delta} - \frac{\mathbf{b}}{\hat{\mathbf{b}}}\mathbf{f}\right) + \boldsymbol{C}\left(\frac{\mathbf{b}}{\hat{\mathbf{b}}} - \mathbf{1}\right)\dot{\mathbf{x}}_d\right] - \mathbf{s}^T\boldsymbol{C}\frac{\mathbf{b}}{\hat{\mathbf{b}}}\mathbf{k}_P\boldsymbol{\sigma} + \nabla \tag{12}$$

where $\nabla = \mathbf{k}_P^T\dot{\mathbf{k}}_P + \mathbf{k}_I^T\dot{\mathbf{k}}_I$ is the adaptation term. With Eq. (12), if $\mathbf{k}_P$ is used for overcome a part of the uncertainties, ∇ can be determined in order to eliminate the rest of them.

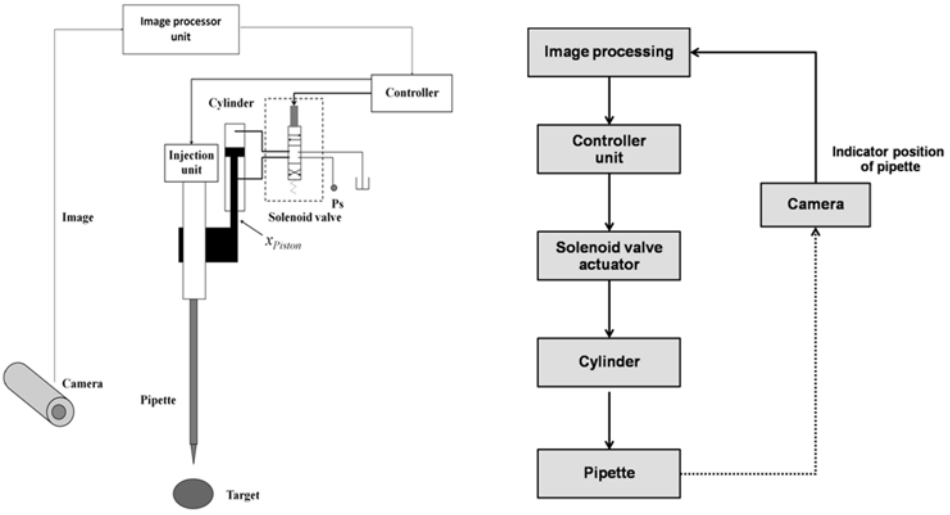

Fig 2: A schematic diagram of position control of an automated pipette with solenoid valve actuator.

To compensate the uncertainties at the beginning state, k_{Pi} should be satisfy as following

$$\|\mathbf{k}_P\| \geq \left\|\left(\frac{\hat{b}}{b}\mathbf{f} + \frac{\hat{b}}{b}\boldsymbol{\delta} - \mathbf{f}\right) + \left(\mathbf{1} - \frac{\hat{b}}{b}\right)\dot{\mathbf{x}}_d\right\| \tag{13}$$

and k_P should be satisfy as follow

$$k_{Pi} \geq |\beta K_O| \tag{14}$$

For $\mathbf{k}_P$, it is corresponding to the gain margin calculation method [29]. Although the proportional term can be designed in order to deal with the first term of Eq. (16), the residual errors still appear. Note that given the differences between the first term and the second term of Eq. (12) is the residual error, thereby it is bounded by a positive value $\Delta = \left\|\boldsymbol{\sigma}^T\left[\boldsymbol{C}\left(\mathbf{f} + \mathbf{b}\boldsymbol{\delta} - \frac{\hat{\mathbf{b}}}{\mathbf{b}}\mathbf{f}\right) + \boldsymbol{C}\left(\frac{\hat{\mathbf{b}}}{\mathbf{b}} - \mathbf{1}\right)\dot{\mathbf{x}}_d\right] - \boldsymbol{\sigma}^T\boldsymbol{C}\frac{\hat{\mathbf{b}}}{\mathbf{b}}\mathbf{k}_P\boldsymbol{\sigma}\right\|$, because of a bounded control input. Adding the bound of the control gain ratio, Eq. (16) can be rewritten as following

$$\dot{\mathbf{V}} \leq -\Delta\boldsymbol{\sigma}^T\boldsymbol{\sigma} - \boldsymbol{C}\frac{\mathbf{b}}{\hat{\mathbf{b}}}\boldsymbol{\sigma}^T\mathbf{k}_I \int \mathbf{s}dt + \mathbf{k}_P^T\dot{\mathbf{k}}_P + \mathbf{k}_I^T\dot{\mathbf{k}}_I \tag{15}$$

or

DRC0005

$$\dot{\mathbf{V}} \leq -\Delta\boldsymbol{\sigma}^T\boldsymbol{\sigma} - \boldsymbol{C}\beta\boldsymbol{\sigma}^T\mathbf{k}_I \int \mathbf{s}dt + \mathbf{k}_P^T\dot{\mathbf{k}}_P + \mathbf{k}_I^T\dot{\mathbf{k}}_{Ii} \quad (16)$$

As the beginning state, the integral term of the adaptation law may be arbitrary small, because the uncertainties at the beginning state are compensated with $\mathbf{k}_P$. For this reason, Eq. (16) can be substituted with the adaptation law and becomes

$$\dot{\mathbf{V}} \leq -\Delta\boldsymbol{\sigma}\boldsymbol{\sigma}^T \quad (17)$$

If $K_T = K_O + K_d + \|\mathbf{u}_{sign}\|$, the adapted of the proportional gain for each sliding surface can be considered as

$$k_{Pi} \geq |\beta K_T| \quad (18)$$

As above control law design, the adaptation law can be determined as $\dot{\mathbf{k}}_P = \beta\boldsymbol{\sigma}^T\mathbf{C}\boldsymbol{\sigma}$ and $\dot{\mathbf{k}}_I = \beta\boldsymbol{\sigma}^T\mathbf{C}\int\boldsymbol{\sigma}dt$. In addition, $\dot{\mathbf{V}}$ in Eq. (17) is negative definite ($\dot{\mathrm{V}} < 0$) and the sliding motion can be guaranteed especially inside the sliding surface.

3 SYSTEM MODELING

As seen in Fig.2, the physical system of an automated pipette injection consists of many complex mechanism and largely nonlinearity phenomenon. The position control of the pipette depends on the regulating piston of the cylinder, while the piston position is direct controlled by adjustable distance of the spool valve of solenoid valve actuator. The distance between the objective and the ending point of the pipette can be measured by an image processing method in which an image is pictured with a camera and is converted into the digital form. The image processor unit will transfers the digital form to the signal condition and sent to the controller unit. For the continuity equation of the automated pipette injection, it can be described as follows.

3.1 Electromagnetic system

To activate the solenoid valve (see Fig. 2), it is controlled with the input current that is used for regulating the electro-magnetic force of the solenoid valve. The relationship between the electro-magnetic attraction force of the solenoid valve and the input current [24] can be obtained by

$$F_{EM} = \frac{L^2 i^2}{N^2 A_e \mu_0} \quad (19)$$

where the electro-magnetic attraction force F_{EM} depend on the input current i, L is the inductance of the magnetic circuit, N is the number of coil turn, A_e is the effective cross section area of flux path, μ_0 is the permeability of air.

3.1 Mechanical system

The mechanical system of the automated pipette injection with a spring-return solenoid valve actuator (see Fig.2) can be considered by the Newton's second law. The electromagnetic force ($\boldsymbol{F_{EM}}$) of a spool in the valve is

$$M_{Spool}\ddot{x}_{Spool} + b_{Spool}\dot{x}_{Spool} + k_{Spool}x_{Spool} = F_{EM} + F_{Pressure} - F_{Friction,spool} \quad (20)$$

$$M_{Spool}\ddot{x}_{Spool} + b_{Spool}\dot{x}_{Spool} = F_{EM} + F_{Pressure} - F_{Spring} - F_{Friction,spool} \quad (21)$$

where b_{Spool} is the damping coefficient of the solenoid valve, k_{Spool} is the spring coefficients of solenoid valve, and $F_{Spring} = k_{Spool}x_{Spool}$ which assume to take the spring pre-tension into account. Note that the stick-slip friction effect during the dynamic of the spool valve is assumed to very small and is ignored for in this work ($F_{Friction,spool} \approx 0$). $F_{Pressure}$ is the pressure force [24] which can be obtained by

$$F_{Pressure} = P_{supply}\Delta A_{in} + P_{out}\Delta A_{out} \quad (22)$$

where ΔA_{in} and ΔA_{out} are the different areas on the surface of spool valve (spool lands) of a solenoid valve actuator, which are affected by P_{supply} and P_{out} in different directions [25]. And due to ΔA_{out} assumes to be zero in general, $F_{Pressure}$ is dominated by P_{supply} and ΔA_{in}. As seen in Fig. 2, the steady-state flow passing the solenoid valve can be approximated as follow [26]

$$Q = k_Q x_{Spool} - k_c P_{Load} \quad (23)$$

where k_Q and k_c are positive constants. Q is the load flow. The continuity equation for the fluid flow in the piston [26] can be derived as

$$Q - A_{Piston}\dot{x}_{Piston} - C_{leakage}P_{Load} = \frac{V}{4\beta_V}\dot{P}_{Load} \quad (24).$$

where $C_{leakage}$ is positive constant. The relationship of dynamic equation for the variable piston of cylinder [26] can be defined by

$$\frac{K_Q}{K_{Spool}}[F_{EM} + F_{Pressure}] - \frac{K_Q}{K_{Spool}}\left[M_{Spool}\ddot{x}_{Spool} + b_{Spool}\dot{x}_{Spool}\right] - K_C\left[\frac{M_{Piston}\ddot{x}_{Piston} + B_{Piston}\dot{x}_{Piston}}{A_{Piston}}\right] - A_{Piston}\dot{x}_{Piston} - C_{leak}\left[\frac{M_{Piston}\ddot{x}_{Piston} + B_{Piston}\dot{x}_{Piston}}{A_{Piston}}\right] - \left[\frac{K_C + C_{leakage}}{A_{Piston}}\right]F_{Friction} = \frac{V}{4\beta_V}\dot{P}_{Load} \quad (25)$$

DRC0005

Considering Eq.(19) to Eq.(25) and Fig.2, the distance between the objective and the ending point of the pipette depends on regulating the piston of the cylinder. For simplification and with the canonical form of the proposed controller design as in Eq. (1), the relationship between the current input and the distance of the piston can be approximated to the first-order differential equation which based on the following assumption [26]:

Assumption 4: the dynamics of solenoid valve are faster than the total dynamic of the system.
Assumption 5: the total of fluid volume of both side chambers of cylinder is too small.
Assumption 6: the mass and the viscous friction force of the spool and the regulating piston are small.

Consequently, by Eq.(19) to Eq.(25), the first-order differential equation based on above assumptions can be defined as follow.

$$A_{Piston}\dot{x}_{Piston} = K_{QS}[F_{EM} + F_{Pressure}] - F_{Spring} - K_{CA}F_{Friction} \quad (26).$$

where K_{QS} and K_{CA} are positive constant. For $F_{Friction}$, it can be considered as the stick-slip friction during the regulating piston of the cylinder. As seen in Eq.(26), due to small difference lands area [22], $F_{Pressure}$ in the solenoid valve is too small compare to the F_{EM} and is neglected for the computation in this work. Thereby, Eq.(26) can be rewritten as

$$A_{Piston}\dot{x}_{Piston} = K_{QS}F_{EM} - K_{CA}F_{Friction} \quad (27).$$

$$\frac{A_{Piston}}{K_{CA}}\dot{x}_{Piston} = \frac{K_{QS}}{K_{CA}}F_{EM} - F_{Friction} \quad (28).$$

Where $\frac{K_{QS}}{K_{CA}}F_{EM} = F_{Drive}$. From Eq.(28), the standard Coulomb plus static plus viscous friction during stick can be defined [27] as

$$F_{Friction} = F_{Slip}(\dot{x}_{Piston})\lambda_{Friction}(\dot{x}_{Piston}) + F_{Stick}(F_{Drive})(1 - \lambda_{Friction}((\dot{x}_{Piston})) \quad (29)$$

and

$$\lambda_{Friction}(\dot{x}_{Piston}) = \begin{cases} 1 & |\dot{x}_{Piston}| > \alpha_{Friction} \\ 0 & |\dot{x}_{Piston}| > \alpha_{Friction} \end{cases} \quad (30)$$

where $\alpha_{Friction} > 0$ is arbitrary small number which restrict a velocity band during sticks state. For simplicity, F_{EM} in Eq.(19) can be approximated [26] as following

$$F_{EM} = K_{EM}i_s \quad (31)$$

where $K_{EM} = \frac{L^2}{N^2 A_e \mu_0}$ is the control input current gain, $i_s = i^2$ is the virtual control input in current square (A^2), while the value of the electro-magnetic force F_{EM} depend on the current input. Therefore, Eq.(28) can be rewritten as

$$\frac{A_{Piston}}{K_{CA}}\dot{x}_{Piston} = F_{Drive} - F_{Friction} \quad (32)$$

Additionally, by Eq. (19) to Eq. (32), it is difficult to obtain the exactly system parameters, because the real system's large complexity [33]. Therefore, with the proposed canonical from of Eq.(1) and for simplification, the approximation system modeling of the real plant based on the process reaction curve method can be defined as

$$\dot{x}_{Piston} = -15x_{Piston} + 145F_{Drive} \quad (33)$$

For validation the system modeling of Eq.(33), it can be seen in Fig. 3. This show the response of the piston displacement by the measurement and the system modeling are similar trajectories in which the validation process was excited with the current input equal to be 0.1 A. Nevertheless, the system modeling of Eq. (33) is not accounted with the effect from the stick-slip friction term $F_{Friction}$. Thus, if $F_{Friction}$ is considered, Eq. (33) can be rewritten as

$$\dot{x}_{Piston} = -15x_{Piston} + 145F_{Drive} - F_{Friction} \quad (34)$$

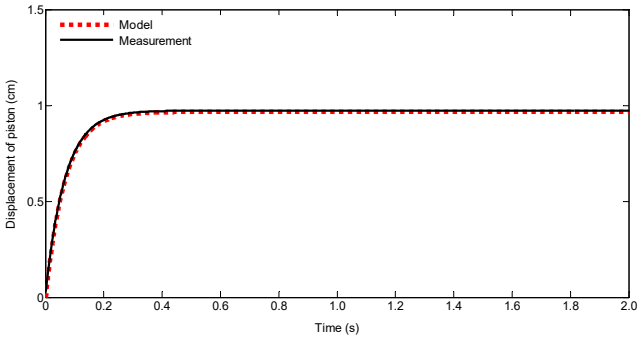

Fig 3: Shows the validity of the system modeling with different current input (A).

Note that due to the development of the proposed control technique is based on the robust control approaches in which have the capability to neglect the need of precise system modeling [34]. Therefore, the system modeling of Eq. (34) can be used for evaluation the performance of the proposed controller design in the simulation tests.

4. RESULTS AND DISCUSSION

For verification the performance of the proposed controller (SMC & Adaptive PI) design, the system modeling of Eq. (34) is used in order to assess the tracking performance of the controller which is performed via Matlab-Simulink programming with a sampling period of 1 ms, while its performance of the proposed controller is compared with the conventional SMC control techniques.

DRC0005

Fig. 4 (a) shows the responses tracking characteristic of the controller. In this task, the friction effect due to the stick-slip is not accounted for assessment the control performance. For the setting control parameters, the value of K_sign for the SMC technique and the proposed control technique are to be 0.5 and 0.005, respectively. For the simulation tests, this shows the proposed controller has a small rise time and setting time, and higher tracking accuracy than the SMC technique. The result shows that the proposed adaptation law is able to update the PI controller online within a short period. Additionally, the proposed control scheme can offer the optimal control input rapidly and has smooth control input (see Fig. 4 (b)) and is capable of stirring the pipette closes to the desired position very well, while the response and the control input of the SMC technique has high chattering phenomena which is affected from the signum function of the SMC technique.

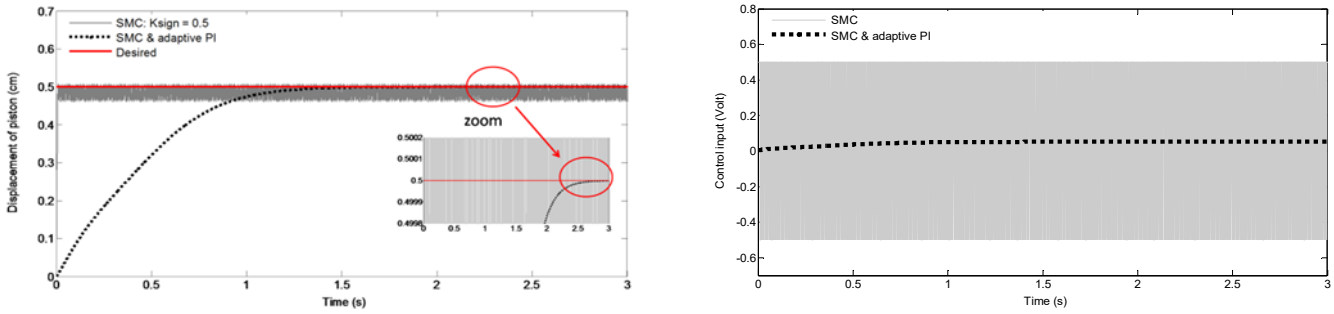

(a) (b)

Fig 4: Comparisons control performance of different control technique (without stick-slip friction).

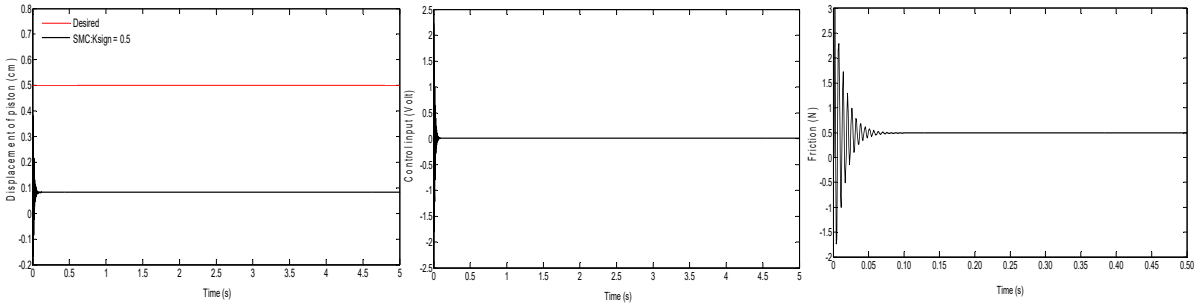

(a) $K_{sign} = 0.5$

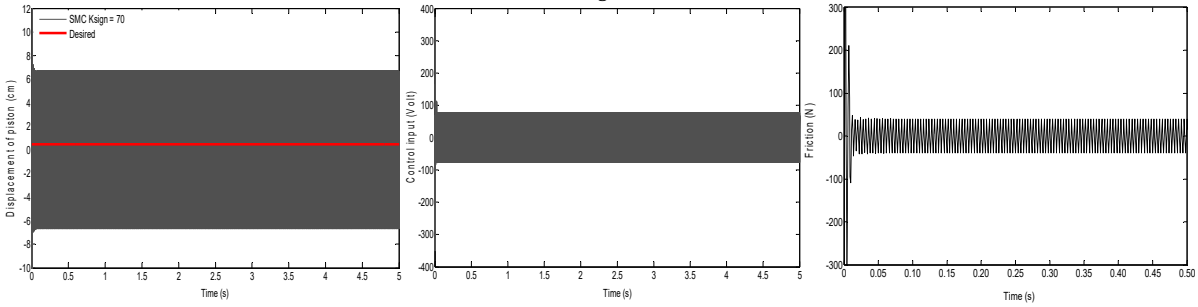

(b) $K_{sign} = 70$

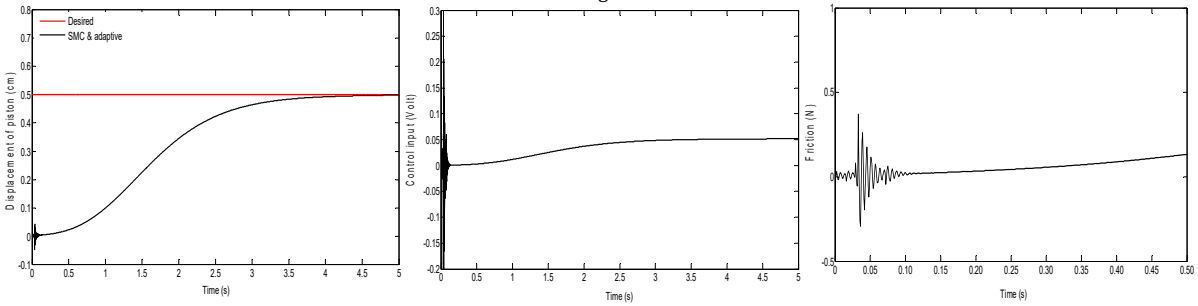

(c) SMC & adaptive PI

Fig 5: Comparison control performance of different control techniques (with stick-slip friction)

Fig. 5 shows the disturbance rejection and the robust control performance comparison between the proposed controller design technique and the SMC technique in which the stick-slip friction effect is chosen to be F_Stick=6N and F_Slip=6N. For assessment the control performance, the values of K_sign for the SMC technique are selected to be 0.5 and 70, while the value of K_sign of the proposed control technique is to be 0.005. The results show that the proposed controller design is capable of compensation the stick-slip friction effect very well as the pipette is capable of stirred to the desired position with tiny effect from the stick-slip friction effect and has high tracking accuracy.

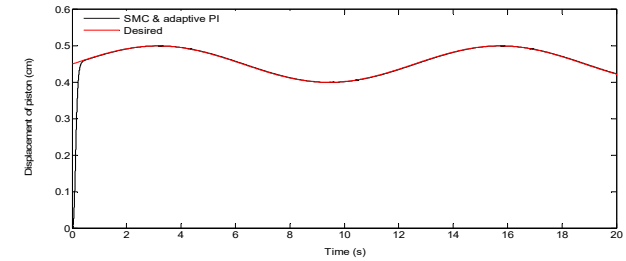

(a)

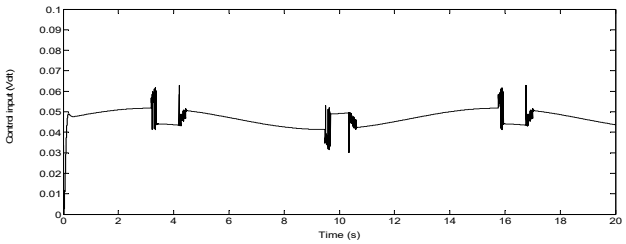

(b)

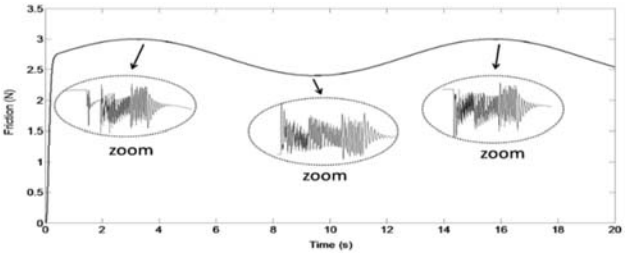

(c)

Fig 6: Comparison control performance of different control technique (with stick-slip friction).

Fig.6 shows the performance assessment of the proposed controller design by vary the desired position. This proposed to confirm the efficiency of proposed control technique, which has high robustness and high tracking accuracy. The results show that the proposed controller is capable of control the position of the pipette closed-to the desired value very well and has tiny effect from the stick-slip friction. Note that since the real system is a rather complex mechanism and large non-linearity. Therefore, the approximating model (Eq.(34)) cannot exactly demonstrate the real plant. Nevertheless, due to the proposed control technique is designed base on the robust control approaches, which have ability to ignore the need for exactly modeling [34]. Therefore, the simulation results based on the approximating model of Eq. (34) can be used in order to assessment the performance of the controllers in this work.

5. Conclusions

The sliding mode control with a new adaptive PI controller technique was used in order to control the motion of an automated pipette injection in microscopic level which requires the high-precision of the movement. The movement of the pipette depends on the distance of the piston of a cylinder, which the piston position depends on the position control of the spool valve in the solenoid valve actuator. The solutions reveal that the proposed control technique is capable to control the position of the pipette closed-to the desired position very well, high robustness, and high tracking accuracy as its response is tiny affected from the friction force (stick-slip).

6. Acknowledgement

This work is supported by the KKU Engineering Research Fund, the Faculty of Engineering, Khon Kaen University.

7. References

[1] Meng, L. (2014), Acceleration Method of 3D Medical Images Registration Based on Compute Unified Device Architecture. Bio-Medical Materials and Engineering, 2014. 24(1): p. 1109-1116.

[2] Li, S., et al. (2001), Automatic analysis of image of surface structure of cell wall-deficient EVC. Bio-Medical Materials and Engineering, 2001. 11(3): p. 159-166.

[3] Huang, H.B., et al. (2009), Robotic Cell Injection System With Position and Force Control: Toward Automatic Batch Biomanipulation. Robotics, IEEE Transactions on, 2009. 25(3): p. 727-737.

[4] Nogawa, K., et al. (2010), Motion control of bacteria-driven micro objects by Nano/Micro pipettes. in Nanotechnology (IEEE-NANO), 2010 10th IEEE Conference on. 2010.

[5] Becattini, G., L.S. Mattos, and D.G. Caldwell (2014), A Fully Automated System for Adherent Cells Microinjection. Biomedical and Health Informatics, IEEE Journal of, 2014. 18(1): p. 83-93.

[6] Yi, Z., T. Kok Kiong, and H. Sunan (2009), Vision-Servo System for Automated Cell Injection. Industrial Electronics, IEEE Transactions on, 2009. 56(1): p. 231-238.

[7] Ahn, K. and S. Yokota (2005), Intelligent switching control of pneumatic actuator using on/off solenoid valves. Mechatronics, 2005. 15(6): p. 683-702.

[8] Zaki, M., A. Aljinaidi, and M. Hamed (2003), Tribological behavior of artificial hip joint under the effects of magnetic field in dry and lubricated sliding. Bio-Medical Materials and Engineering, 2003. 13(3): p. 205-221.

[9] Hodgson, S., et al. (2015), Nonlinear Discontinuous Dynamics Averaging and PWM-Based Sliding Control of Solenoid-Valve Pneumatic Actuators. Mechatronics, IEEE/ASME Transactions on, 2015. 20(2): p. 876-888.

[10] Utkin, V.I. (1993), Sliding mode control design principles and applications to electric drives. Industrial Electronics, IEEE Transactions on, 1993. 40(1): p. 23-36.

[11] Huang, Y.J. and T.C. Kuo (2005), Robust output tracking control for nonlinear time-varying robotic manipulators. Electrical Engineering, 2005. 87(1): p. 47-55.

[12] Hajatipour, M. and M. Farrokhi (2010), Chattering free with noise reduction in sliding-mode observers using frequency domain analysis. Journal of Process Control, 2010. 20(8): p. 912-921.

[13] Xu, Y. (2008), Chattering Free Robust Control for Nonlinear Systems. Control Systems Technology, IEEE Transactions on, 2008. 16(6): p. 1352-1359.

[14] Lee, H. and V.I. Utkin (2007), Chattering suppression methods in sliding mode control systems. Annual Reviews in Control, 2007. 31(2): p. 179-188.

[15] Shahnazi, R., H.M. Shanechi, and N. Pariz (2008), Position Control of Induction and DC Servomotors: A Novel Adaptive Fuzzy PI Sliding Mode Control. Energy Conversion, IEEE Transactions on, 2008. 23(1): p. 138-147.

[16] Guan, C. and S. Pan (2008), Adaptive sliding mode control of electro-hydraulic system with nonlinear unknown parameters. Control Engineering Practice, 2008. 16(11): p. 1275-1284.

[17] Zhang, X., X. Liu, and Q. Zhu (2014), Adaptive chatter free sliding mode control for a class of uncertain chaotic systems. Applied Mathematics and Computation, 2014. 232(0): p. 431-435.

[18] Li, J. and L. Yang (2014), Adaptive PI-Based Sliding Mode Control for Nanopositioning of Piezoelectric Actuators. Mathematical Problems in Engineering, 2014: p. 10.

[19] Akbarzadeh, T.M.R. and R. Shahnazi. Direct adaptive fuzzy PI sliding mode control for a class of uncertain nonlinear systems. in Systems, Man and Cybernetics, 2005 IEEE International Conference on. 2005.

[20] Chang, W.-D. and J.-J. Yan (2005), Adaptive robust PID controller design based on a sliding mode for uncertain chaotic systems. Chaos, Solitons & Fractals, 2005. 26(1): p. 167-175.

[21] Kuo, T.C., et al. (2008), Adaptive sliding mode control with PID tuning for uncertain system. Engineering Letters, 2008.

[22] Howell, M.N. and M.C. Best (2000), On-line PID tuning for engine idle-speed control using continuous action reinforcement learning automata. Control Engineering Practice, 2000. 8(2): p. 147-154.

[23] Hsu, C.-F. and B.-K. Lee (2011), FPGA-based adaptive PID control of a DC motor driver via sliding-mode approach. Expert Systems with Applications, 2011. 38(9): p. 11866-11872.

[24] Taghizadeh, M., A. Ghaffari, and F. Najafi (2009), Modeling and identification of a solenoid valve for PWM control applications. Comptes Rendus Mécanique, 2009. 337(3): p. 131-140.

[25] Garcia, C. (2008), Comparison of friction models applied to a control valve. Control Engineering Practice, 2008. 16(10): p. 1231-1243.

[26] Kim, C.S. and C.O. Lee (1996), Speed control of an overcentered variable-displacement hydraulic motor with a load-torque observer. Control Engineering Practice, 1996. 4(11): p. 1563-1570.

[27] Liyu, C. and H.M. Schwartz. Stick-slip friction compensation for PID position control. in American Control Conference, 2000. Proceedings of the 2000. 2000.

[28] Hrovat, D. and J. Sun (1997), Models and control methodologies for IC engine idle speed control design. Control Engineering Practice, 1997. 5(8): p. 1093-1100.

[29] Slotine, J.J. and W. Li (1991), Applied Nonlinear Control. 1991: Prentice-Hall, Englewood Cliffs, NJ.

[30] Jian-Xin, X., P. Ya-Jun, and L. Tong-Heng (2004), Sliding mode control with closed-loop filtering architecture for a class of nonlinear systems. Circuits

and Systems II: Express Briefs, IEEE Transactions on, 2004. 51(4): p. 168-173.

[31] Utkin, V. (1997), Variable structure systems with sliding modes. Automatic Control, IEEE Transactions on, 1977. 22(2): p. 212-222.

[32] Radpukdee, T. and P. Jirawattana (2009), Uncertainty learning and compensation: An application to pressure tracking of an electro-hydraulic proportional relief valve. Control Engineering Practice, 2009. 17(2): p. 291-301.

[33] Jansri, A. and P. Sooraksa (2012), Enhanced model and fuzzy strategy of air to fuel ratio control for spark ignition engines. Computers & Mathematics with Applications, 2012. 64(5): p. 922-933.

[34] Richard, C.D. and H.B. Robert (2011), Modern control systems. 2011: Upper Saddle River, N.J.: Prentice Hall.